Filamin cross-linkers as rheology regulators in F-actin networks

B.A. DiDonna
Institute for Mathematics and its Applications, University of Minnesota, Minneapolis, MN 55455-0436, USA

Alex J. Levine
Department of Chemistry and Biochemistry, University of California, Los Angeles, CA 90095, USA

(Dated: December 7, 2005)

We report on the nonlinear mechanical properties of a statistically homogeneous, isotropic semiflexible network cross-linked by polymers containing numerous small unfolding domains. This model captures the main mechanical features of F-actin networks cross-linked by filamin proteins, which contain twenty-four such Ig-domains that may unfold under applied strain. We show that under sufficiently high strain the network spontaneously organizes itself so that an appreciable fraction of the filamin cross-linkers are at the threshold of domain unfolding. We discuss via a simple model the cause of this network organization and suggest a qualitative experimental signature of this network reorganization under applied strain that may be observable in intracellular microrheology experiments of Crocker *et al.*.

PACS numbers: 87.16Ka, 82.35.Rs, 62.20.Dc

I. INTRODUCTION

The cytoskeleton of eukaryotic cells can be described as a biopolymer gel or cross-linked network[1, 2, 3]. The microstructure of this network fundamentally differs from better understood polymer gels. In these well-studied synthetic systems the mean distance between cross-links along a constituent polymer chain is much longer than the distance over which the chain tangents remain correlated, *i.e.* the thermal persistence length of the polymers [4]. These synthetic networks can be thought of as assemblies of cross-linked random walks. The principal constituent of the cytoskeleton, however, is a stiff protein aggregate, F-actin that is cross-linked densely on the scale of its own thermal persistence length. The cytoskeleton is better described as a cross-linked network of flexible but essentially straight filaments rather than by interconnected random walks.

A number of researchers have begun to explore the quantitative relation between the novel microstructure of this biopolymer gel to its observed mechanical properties [5, 6, 7]. More recently, it has been proposed that, due to their different microstructure, these *semiflexible gels* have macroscopic linear moduli that are generically more sensitive to their chemical composition [9, 10, 11, 12, 13, 14] than traditional flexible gels. Their response to point forces over mesoscopic distances are much more complex than suggested by the predictions of continuum elasticity[15]. In addition they exhibit a highly tunable (through network microstructure) nonlinear response to stress[16].

The current understanding of the complex relationship between the network architecture on the nanoscale and the long-length scale mechanical properties relies only on semiflexibility of the filaments that are assumed to be cross-linked irreversibly by cross-linking agents, which exert arbitrary constraint forces required to prevent slip between the filaments at a cross-link. The cytoskeleton of living cells, on the other hand, is vastly more complex than the model semiflexible network systems studied. The constituent filaments in the cytoskeleton are polydisperse in length, and, through bundling interactions, have a variety of cross-sectional radii and hence bending moduli. Furthermore these filaments are cross-linked by a plethora of highly structured proteins that play an active role in the generating internal stresses and in sensing externally imposed stress.

There has recently been a great deal of interest in a class of cross-linkers that contain unfolding domains such as α-actinin[17, 18] and filamin[19, 20]. Such cross-linkers have protein domains along their backbone that unfold reversibly at a critical pulling force. It is still a matter of debate what the function of these domains may be, but one may speculate that by exposing new chemical groups in the unfolded domains, cross-linking agents such as filamin may play a role in transducing externally local network strain into biochemical signals.

In this paper we investigate the purely mechanical effect of cross-linkers such as filamin that have unfolding domains. Clearly, the mechanical effect of filamin–domain unfolding occurs only at some finite applied stress so the effect we wish to study is evident only in the nonlinear elastic response of the material observed under finite strain conditions. In this aspect the present work differs from much of the recent theoretical research on semiflexible network mechanics that focused on the linear response regime.

We show that for a sufficiently stretched gel, the population of cross-links at given tension grows exponentially up to the unfolding force of the domains. Thus at moderate applied stresses the system appears to self-consistently adjust is mechanical properties so as to achieve a strain state in which a significant fraction of its cross-linkers are poised at the unbinding transition of their internal domains. The evolution of this high susceptibility state in which the system responds to small stress

fluctuations with anomalously large strain fluctuations may contribute to the low-frequency intracellular strain fluctuations as measured by Hoffman *et el.*[21]. These microrheological measurements suggest the presence of the nonthermal enhancement of low-frequency strain fluctuations. Such fluctuations may be understood in terms of the network generically evolving into this high susceptibility state under the action of internal molecular motors (*e.g.* myosin – not considered in our model) so that either small fluctuations in motor protein activity or Brownian fluctuations of the network leads to the coordinated unfolding of numerous filamin cross-linkers and a consequent large-scale cytoskeletal arrangement event.

The remainder of this article is arranged as follows. In section II we discuss the our numerical model of the filamin cross-linked F-actin network. We present the results of this modeling in section III before developing a simple analytic approach to explain the observed phenomenon. Finally we conclude in section IV where we discuss the generality of our results and place them in the broader context of the mechanics of semiflexible gels in general and the modeling of the cytoskeleton in particular.

II. THE MODEL

We develop a simple model of a statistically homogeneous, isotropic network of semiflexible filaments in two-dimensions. These networks are formed by the random deposition of straight filaments of equal length within the simulation box in a manner identical to that of Head *et al.*[9, 11, 12], *i.e.* by placing straight rods of a fixed length at random positions and orientations in a box with periodic boundaries. At points where two rods intersect a node is added to each rod and a cross-linker is added connecting the nodes. The cross-linkers have zero rest length. Rods are added until the average number of cross-links per rod reaches a predetermined target value that we use to parameterize the network density. A model network constructed by the procedure described above is shown in Figure 1. The sections of rod between nodes are modeled as linear springs with fixed elastic constant *per unit length* of rod. The cross-linkers exert no constraint torques at the nodes so that the rods are free to bend there with no energy cost. We write the Hamiltonian for each filament as

$$\mathcal{H} = \frac{1}{2}\mu \int \left(\frac{\mathrm{d}l(s)}{\mathrm{d}s}\right)^2 \mathrm{d}s\,, \qquad (1)$$

where $dl(s)/ds$ gives the strain or relative change in local contour length, and μ is the Young's modulus of the filament (essentially a spring constant normalized to 1/[length]).

We do not include filament bending in the numerical model. This omission results is a computational advantage owing to the reduction of number of degrees of freedom necessary to monitor the deformation state of an individual semiflexible filament. This computational advantage prevents us from accurately modeling the linear response of the network. For example, in the linear response of the cross-linked semiflexible network there is an abrupt transition with increasing network density in the mode of energy storage from a dominance of bending modes to stretching modes. We will not observe this effect. We concentrate on the non-linear, finite extension regime where the effects of the internal structure of the cross-links become evident. The behavior of semiflexible networks with freely rotating cross-links has been shown to be dominated by semiflexible filament stretching instead of bending [22] so we expect to accurately capture the nonlinear behavior of the composite network with our restricted model for the elasticity of the semiflexible filaments.

Similarly we anticipate that the results derived here are essentially independent of network dimensionality since network connectivity, not the dimensionality of the space in which the network is embedded should control

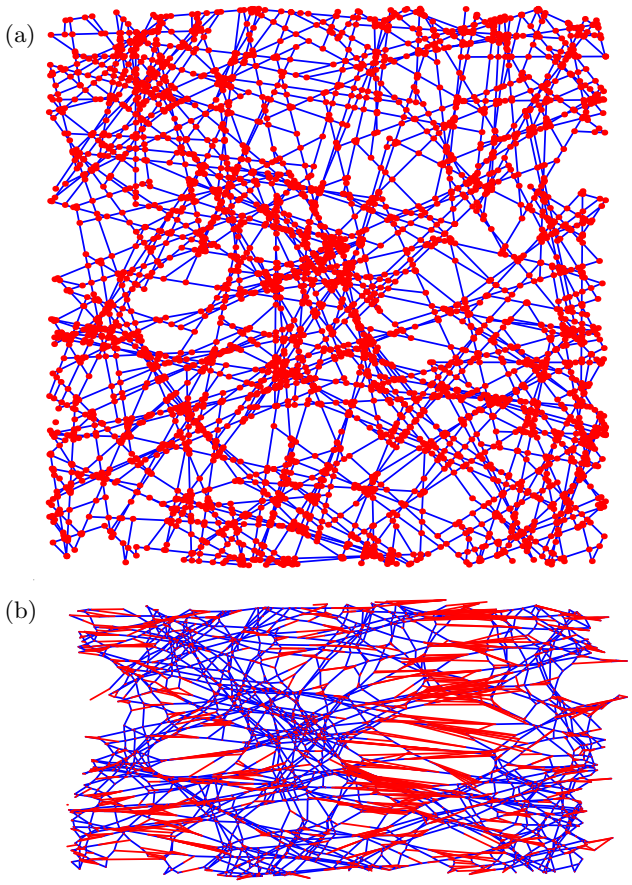

FIG. 1: (Color Online) Model network showing the F-actin filaments in blue and the filamin cross-linking agents in red. (a) shows the unstrained network as constructed by random deposition of the filaments in the two-dimensional simulation box. (b) shows the same network under affinely imposed uniaxial extension. The extension direction is along the x-axis. The magnitude of the strain in this case is 100%.

the collective mechanical properties of the system. It must be noted that steric interactions between noncross-linked filaments may contribute to the moduli in three dimensions. At low network densities we expect these steric effects to be subdominant. The validity of both of these simplifying assumptions can be directly tested in future work where dependence of our results upon filament bending elasticity and on network dimensionality will be explored.

Since the filamin cross-linkers are small flexible polymers, their elasticity is essentially that of a worm-like chain[23]. The equilibrium activation force for the unfolding of the internal Ig-domains of the protein is high enough to place it well away from the linear regime on the force extension curve of the filamin. Thus in equilibrium Ig-domain unfolding occurs at an extension nearly equal to the contour length of the filamin polymer so that the entropic force is approximately $f \sim 1/(\ell - \ell_f)^2$. When an Ig domain unfolds the contour length of the filamin increases, adding enough length to the polymer to relax most of the tension at fixed extension.

We model the force extension curve of a single cross-linker as a simple sawtooth. Each branch of the sawtooth represents the entropic elasticity of a cross-linker with a fixed number of unfolded domains. For simplicity, we take the additional contour length generated during any unfolding event ℓ_f to be a constant and the force–extension relation on each branch of the sawtooth to be linear with spring constant k_f. Thus the maximum force on each branch of the sawtooth, $k_f\ell_f$, corresponds to the critical unfolding force of a domain. We neglect the rate-dependence of this unfolding force[24] that is found in nonequilibrium unfold dynamics. Though the physiological filament cross-linkers have a finite number of unfolding domains (24), we will take our sawtooth force extension curve to have an infinite number of branches. In doing so we ignore the stretching–rate dependence of our mechanical measurements as well as the eventual strain-hardening of the material when all the Ig-domains of the cross-linking filamin molecules have been unfolded at extremely large strain amplitudes.

We find equilibrium states of the simulated network through straightforward force balancing. The network is subject to stepwise shear or uniaxial extension by adjusting the periodic boundaries. At the beginning of each strain step, all nodes are moved affinely to match the change in boundaries. Then the node positions are relaxed through a conjugate gradient routine to a point of local force equilibrium.

Since the cross-linker force extension curve is a sawtooth, there are many possible equilibrium states of the network, corresponding to force equilibration on different branches of the sawtooth. We wish to consider the history dependent states of a strained network, which would in principle require us to use strain steps with displacements smaller than the sawtooth length ℓ_f. However, such a procedure would prove too cumbersome for the large strains and small ℓ_f we wish to consider. Instead,

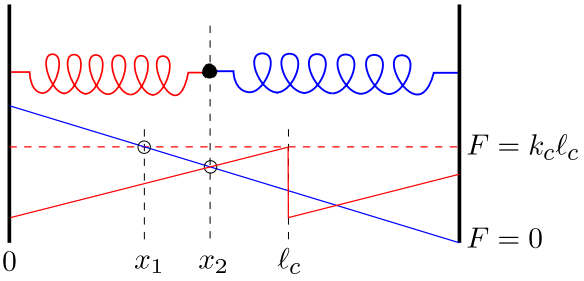

FIG. 2: (Color Online) Conceptual model for action of filamin cross-linkers. The filamin is represented by a nonlinear spring (left), and the rest of the network is approximated as a linear spring (right). The springs are attached in series with the free ends held in a fixed position. Below the springs we plot the force exerted by each spring as a function of the position of the meeting point. The position of force equilibrium between the effective network spring and a flat filamin force is given by point x_1, at the intersection of the dashed red line (flat filamin force) and solid blue line (effective network force). The position of force equilibrium between the effective network spring and a sawtooth filamin force is given by point x_2, at the intersection of the solid red line (sawtooth filamin force) and solid blue line. The downward slope of the effective network force curve necessitates that x_1 and x_2 be on the same sawtooth branch.

we use a two–step equilibration procedure that relaxes the system to a state close to the true history dependent state in terms of minimizing the total length of all cross-links, but also allows for large strain steps. In the first equilibration step, we replace the sawtooth force law for all cross-linkers by the following force law:

$$\mathbf{f} = \begin{cases} k_f\mathbf{x} & |\mathbf{x}| < \ell_f, \\ k_f\ell_f & |\mathbf{x}| \geq \ell_f. \end{cases} \tag{2}$$

Thus, beyond the first sawtooth length, a cross-linking filamin molecule exerts a constant contractile force of magnitude $k_f\ell_f$. The combined network of linear elastic rods and constant force cross-links is equilibrated. Finally, we reimpose a sawtooth force law for the cross-linkers and equilibrate the network a second time.

If all the cross-linkers acted independently, then on the final step of equilibration described above each cross-linker would reach force balance on the earliest possible sawtooth branch (smallest total cross-link extension). The argument for this claim is illustrated in Figure 2. When the constant force law is replaced by a sawtooth, the rest of the network will exert a net force that extends the cross-link. However, the cross-link will not extend to its next sawtooth branch, since as it relaxes the network can only exert a total force less than $k_f\ell_f$. Conversely, since the rest of the network was originally equilibrated at the critical pulling force, then it is extended as far as it can be by the cross-linker, thus the cross-linker is on the earliest possible branch of the sawtooth for which it could establish force equilibrium with the rest of the network. In practice, collective relaxations of the network push in-

dividual cross-links onto different sawtooth branches in this final step. However, we found that for a variety of strain step sizes the quantitative behavior discussed in the next section was identical.

III. SIMULATION RESULTS

We present data for networks with a filament density such that there are on average 30 cross-links per rod. The rods have a unique length of $\ell_R = 0.2$ measured in units of the length of the unstrained, square simulation box. This gives an average crosslink separation of $\ell_c \approx 6.6 \times 10^{-3}$ in simulation units. For these values we find negligible system-size effects. Hereafter we measure the network density (n number of rods per unit area) in terms of the mean distance between cross-links ℓ_c. It can be shown that $\ell_c \simeq \pi/\left(2n\ell_R^2\right)$[11]. The other length scales in the system is the contour length generated in a single Ig-domain unfolding event ℓ_f, which we take to be the length of the saw-tooth in our approximate form of the cross-linker force-extension relation. We found that for $\ell_c/\ell_R \gtrsim 15$ and ℓ_f/ℓ_c constant, the network behavior is independent of ℓ_R. We did not have the computational resources to fully investigate the phase space of the ratio ℓ_f/ℓ_c; this we leave for a more detailed study. In this article, we present data primarily for $\ell_f = 1.3 \times 10^{-4}$, or $\ell_f/\ell_c = 0.02$. The distance between crosslinks in physiological f-actin solutions has been quoted as $\ell_c = 0.1\ \mu m$ [25]. Filamin crosslinks have a folded length of 200 nm [26], and each unfolding domain adds $\ell_f = 21\ nm$ of length [27]. Thus the physiological ratio is closer to $\ell_f/\ell_c = 0.2$. We chose the smaller value of ℓ_f/ℓ_c because it enhanced the effects we were measuring – initial simulational studies we have performed for physiological values of ℓ_f/ℓ_c found qualitatively similar results, but the onset of non-linear effects occurred at higher strain values [33]. We will discuss quantitative differences for physiological values of ℓ_f/ℓ_c where appropriate in the following sections.

Finally there are two energy scales in the system determined by the extensional modulus of the filaments μ and the spring constant of the cross-linkers. To fix the energy scale in the problem we set the extensional modulus of the filaments to unity. The average spring constant for a filament segment can then be determined from the mean distance between cross-links, or, in other words, the network density: $k_R = 1/\langle \ell_c \rangle = 150$. In terms of our defined length and energy units, the range of cross-linker spring constant values reported here was in the range $1 \times 10^1 < k_f < 1 \times 10^4$.

A. Elastic moduli

Since we have omitted the bending rigidity of the filaments, these networks necessarily have vanishing elastic moduli in their unstrained state[28]. The networks im-

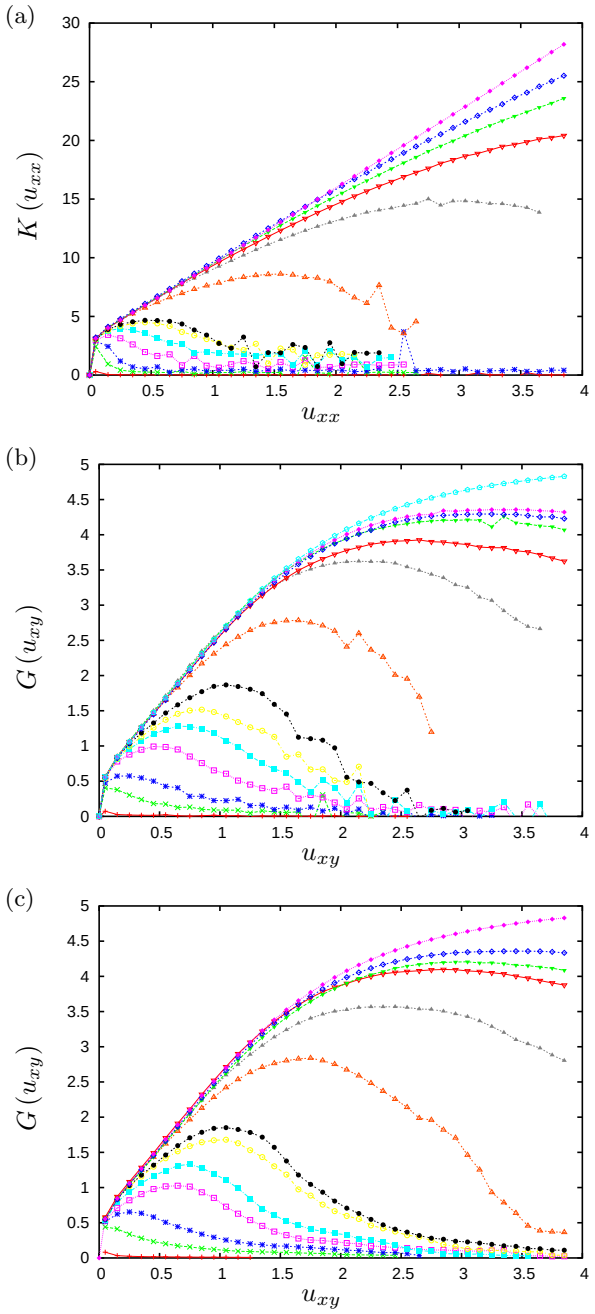

FIG. 3: (Color Online) Differential moduli versus strain for several different cross-linker spring constants k_f and constant cross-link sawtooth length $\ell_f = 1.3 \times 10^{-4}$. (a) Bulk modulus versus uniaxial extensional strain. (b) Shear modulus versus shear strain. (c) Shear modulus versus shear strain, for constant cross-linker force $f = k_f \ell_f$. ¿From lowest to highest curves in each graph, the filamin spring constants are respectively 10, 100, 200, 400, 600, 800, 1000, 2000, 4000, 6000, 8000, 10000 and inextensible crosslinks. (From Section III, the average filament segment spring constant in these units is $\langle k_R \rangle \approx 150$.)

mediately develop non-zero moduli under any imposed finite strain. To characterize the nonlinear mechanical properties of the network we then measure the differential moduli $\partial\sigma_{ij}/\partial u_{ij}$ under any finite applied strain. Figure 3 shows how the bulk and shear moduli evolve as a function of applied strain. The differential moduli all vanish for zero applied strain. Upon increasing applied strain, they grow monotonically to some maximum where the network is stiffening most dramatically under further strain increments. At still larger values of the applied strain, the stress plateaus so that the differential moduli shown here decay to zero. In part (a) of Figure 3 we show the differential bulk modulus $K(u_{xx})$ as computed from the additional uniaxial extension of the network already under strain u_{xx} while in part (b) of this figure we show the differential shear modulus $G(u_{xy})$. From a comparison of these measurements we determine the effective Poisson ratio ν as function of applied strain[29] using

$$\nu = \frac{1}{2}\frac{3K - 2G}{3K + G}. \tag{3}$$

For intermediate deformations, while the network is stiffening, the scale of K is about four times that of G, so $\nu \approx 0.38$.

The underlying cause of this peak in the modulus can be understood from Figure 1(b), which shows a cluster of highly extended cross-linkers that has percolated across the network. Evidently from this figure we can approximate the compliance of the network as the compliance of a composite system. One part of the composite is the filament dominated parts of the network in which the cross-linkers are not greatly extended and the other part is the region of large cross-linker stretch. The effective modulus of the composite system can then be approximated as two nonlinear springs in series.

The force law for the filament dominated parts of the network can be inferred from the top curve in Figure 3(b), which shows the differential shear modulus for networks with non-compliant crosslinks. The shear modulus increases steadily at low shear as the individual filaments align with the shear direction. Above 200% strain, the modulus starts to plateau. In the limit of complete shear alignment, all the filaments lie in direction

$$\frac{u_{xy}\hat{x} + \hat{y}}{\sqrt{u_{xy}^2 + 1}},$$

which asymptotes to $\hat{x}$ for large shear, and have length $\sqrt{u_{xy}^2 + 1} \to u_{xy}$ for large shear. Thus at high shear the extension of individual filaments is linear in the shear and the modulus is constant, with value $G(u_{xy}) = n_{ave}k_R$, where n_{ave} is the average number of filaments per unit cross sectional length. At low and intermediate values of the shear, the differential modulus is observed to grow approximately linearly in shear, up to the maximum value given above.

In contrast, the part of the network dominated by highly extended crosslinks can only sustain a finite maximum stress per unit area, since each crosslinker can only excert a maximum force of $k_f\ell_f$. In the limit of complete shear alignment, the maximum stress is given by $\sigma_{max} = n_{cr}k_f\ell_f$, where n_{cr} is the number of filamin per unit cross-sectional length which take part in the crazing, or splitting, of the network. n_{cr} is determined by the shortest percolation path across the network. The expression for the maximum stress implies that the crazing, and therefore the differential modulus of the network near its maximum, is determined by the product $k_f\ell_f$. Indeed, Figure 3(c) shows the modulus for sheared network where the cross-linker force law is simply that given in Eq. 2 without imposing the sawtooth force law at any step. The curve is nearly identical to Figure 3(b), where the sawtooth force law was imposed at each step. The high extension part of the force law in Eq. 2 is independent of extension, so the differential modulus $\partial\sigma_{ij}/\partial u_{ij}$ is zero.

The composite system of filament and crosslinker dominated regions act as two effective springs in series. The maximum differential shear modulus occurs at the crossover point when the applied stress approaches $n_{cr}k_f\ell_f$. For small k_f/k_R, the crossover occurs in the linear growth region of the differential modulus, where $\sigma_{xy} \sim n_{ave}k_R u_{xy}^2$, so the shear at maximum scales as $u_{xy}^{max} \sim \sqrt{k_f/k_R}$. For larger k_f/k_R the crossover occurs in the region of constant differential shear modulus, so the shear at maximum scales as $u_{xy}^{max} \sim k_f/k_R$.

Though not shown, we also found results identical to Figure 3(c) for the same values of $k_f\ell_f$ when the value of ℓ_f was ten times smaller. The curves were somewhat different for physiological values of ℓ_f/ℓ_c, with ℓ_f ten times larger than for the data presented here. For larger realtive values of ℓ_f the splitting of the network, and therefore the dropoff of the differential moduli, was suppressed at lower shear values, and did not occur till a finite fraction of the filamin population were stretched beyond their initial sawtooth length ℓ_f. Still, in the limit of large strain, the modulus is mainly determined by the combination $F_{max} = k_f\ell_f$. In the next section we will show that most stretched cross-linkers reach equilibrium near $F = F_{max}$, so it is natural that the network elastic response is essentially that of the response of a network with constant force cross-linkers.

B. Cross-linker extension statistics

In Figure 4 we present data on the distribution of cross-linker extensions in mechanically equilibrated networks. Figure 4(b) and (c) show the distributions of cross-link lengths for a representative sample with crosslinks sawtooth length $\ell_f = 1.3 \times 10^{-4}$ and spring constant $k_f = 600$. In Figure 4(b) the distribution of total crosslink lengths for a given value of applied shear is roughly power law. However, when the extension is plotted modulo ℓ_f, as is done in Figure 4(c), the difference between the extension of the cross-linker and the edge of

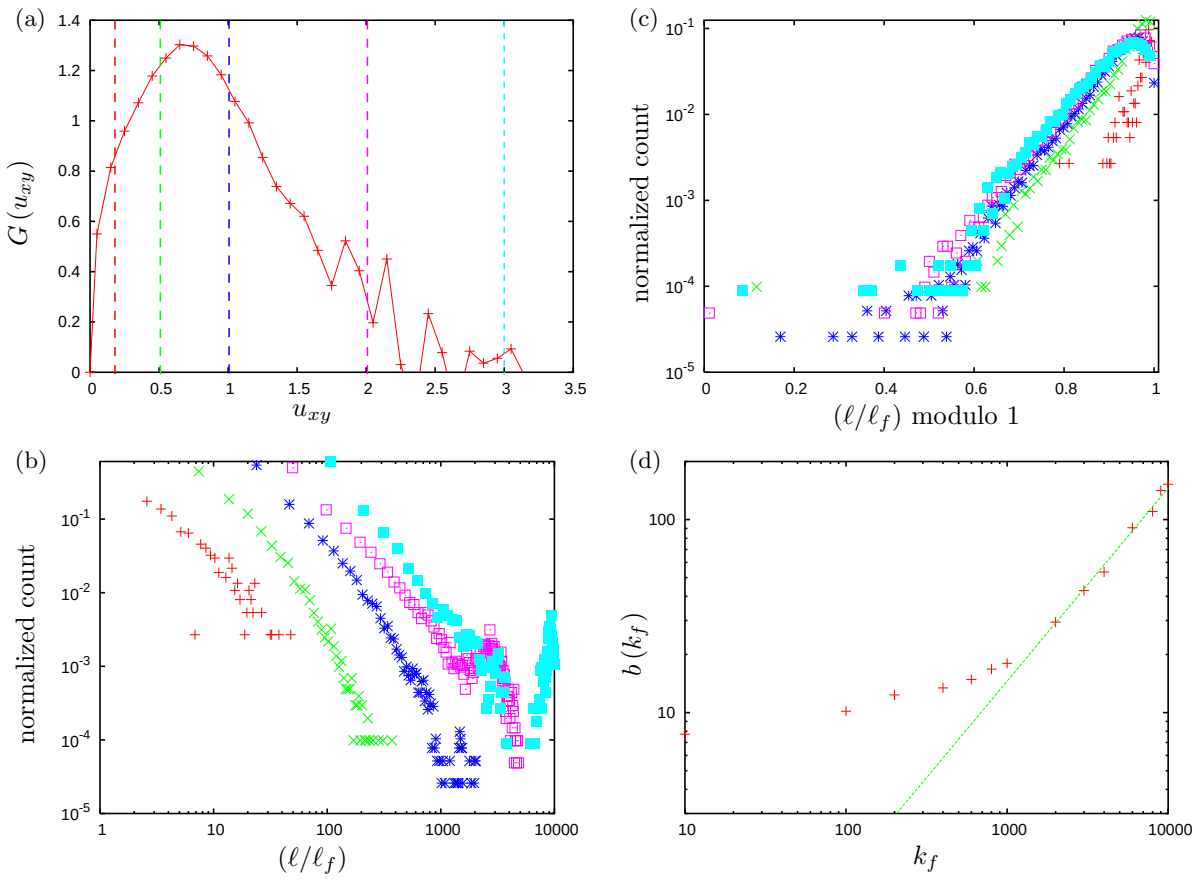

FIG. 4: (Color Online) (a) Shear modulus versus strain for $k_f = 600$ (from Figure 3). (b) Distribution of normalized cross-linker lengths ℓ/ℓ_f in equilibrated networks with $k_f = 600$. Only cross-linkers for which $\ell > \ell_f$ were counted. Each line is for a different value of applied shear. From left to right the corresponding shear values are respectively 0.20, 0.50, 1.00, 2.00, and 3.00 (these shear values are mark with color coded lines in (a)). (c) Distribution of normalized cross-linker lengths ℓ/ℓ_f modulo 1 in equilibrated networks with $k_f = 600$. Data sets are the same as for (b). The exponential parts of the normalized cross-linker length distributions modulo 1 for all values of k_f were fit to $a \exp\left(b(k_f)\ (\ell - \ell_f)/\ell_f\right)$. Plot (d) shows the best fit value of $b(k_f)$ versus k_f. For $k_f > 10^3$, $b(k_f)$ scales roughly as $k_f^{1.33}$ (solid line), whereas for lower values the dependence on k_f becomes weaker. (From Section III, the average filament segment spring constant in these units is $\langle k_R \rangle \approx 150$.)

its nearest saw-tooth step in the force-extension relation shows an entirely different distribution. Once a cross-link has been stretched past its initial sawtooth branch, it tends to reach equilibrium near the high force edge of whichever sawtooth branch on which it comes to rest.

Making this qualitative observation more quantitative, we note that the statistical weight for finding a cross-link extension (modulo ℓ_f) is exponentially enhanced towards length ℓ_f. Moreover, Figure 4(c) shows that once the network is sufficiently strained the exponential enhancement of the statistics grows but the characteristic length of the exponential remains constant.

Figure 4(d) shows data (red crosses) for fits of the length distribution modulo ℓ_f to an exponential functional form

$$a\, e^{\{b(k_f)\ [\ell-\ell_f]/\ell_f\}}.$$

In this graph we plot the fitted value b as a function of filamin spring constant k_f. We found the factor $b(k_f)$ is weakly dependent upon k_f for values of k_f less than $\langle k_R \rangle$, the average filament segment spring constant. $b(k_f)$ approaches a power law dependence on k_f with exponent approximately 1.33 for values greater than $10 \times \langle k_R \rangle$. For $k_f \geq 8 \times 10^3$ the length distribution modulo ℓ_f grows super-exponentially at the highest values, between $0.95\ell_f$ and ℓ_f, so the exponential fit is only approximate.

The appearance of this exponential pile-up in the histogram of filamin extensions is the principal result of this work. We refer to subpopulation of the filamin cross-linkers that make up the exponential tail of the histogram as the *critical cross-linkers*. These numerical data demonstrate that the system approaches a state of nearly maximal fragility in which small stress fluctuations due to either thermal or nonthermal (*i.e.* molecular motor induced) forces can generate large changes in the strain field due to the coordinated rupturing of numerous critical filamin Ig-domains. The response of the system to such stress fluctuations will depend on the spatial dis-

tribution of the critical cross-linkers as well as on the interaction of the critical cross-linkers mediated by the elastic deformation field of the network; these issues will be explored in a future work [30]. Before we address the details of large amplitude strain fluctuations due to the formation of the critical cross-linker population, we explore via a simple analytic model the origin of critical subpopulation in a manner than neglects spatial correlations in the positions of these critical cross-linkers.

To understand the growth of the critical cross-linker subpopulation, where each member is under a force close to the critical force $f_{max} = k_f \ell_f$, we consider a mean-field model for the behavior of a single cross-link in an effective elastic medium representing the rest of the network. We focus on the final phase of the cross-link plus effective network relaxation, where the single cross-link under consideration comes to rest on a particular branch of the force extension sawtooth. The surrounding effective medium acts as a single spring with a linear force–response characterized by the spring constant k_{eff}. The cross-linker is connected in series with the effective network spring, and we fix the total strain of the two-spring system by fixing the free ends. This simplified two-spring model is represented pictorially in Figure 2.

Considering this figure, we have argued that under the correct stress-loading-dependent history of the strain in the effective two-spring system, the filamin spring will come to equilibrium on the same branch of the sawtooth extension curve as it would have if the effective network spring were simply pulled with constant force $F_c = k_f \ell_f$. In Figure 2, we label the position where the pulling force of the effective network spring equals $k_f \ell_f$ as point x_1. We label the position where the effective network spring is in force balance with the sawtooth cross-link force as point x_2. We can solve for the force on both springs at point x_2:

$$\begin{aligned} F &= k_f x_2 \\ &= k_f \ell_f - (x_2 - x_1) k_{eff} \end{aligned} \tag{4}$$

and using these two equalities we determine x_2 in terms of the parameters k_f, ℓ_f and the as yet unknown effective spring constant of the surrounding medium k_{eff}.

$$x_2 = \frac{k_f \ell_f + k_{eff} x_1}{k_f + k_{eff}}. \tag{5}$$

From the above results we calculate the probability distribution of x_2, the final cross-link length modulo ℓ_f. Noting that the above force balance condition determines k_{eff} for any given values of $x_{1,2}$, we write the probability distribution of x_2 in terms of the probability distribution for x_1 while requiring that k_{eff} satisfy Eq. 5 for each pair of stretching lengths $x_{1,2}$. We write $P_2(x_2)$ in terms of the appropriate integral over the probability distribution $P_1(x_1)$ and the distribution $K(k_{eff})$ over all possible spring constants of the effective medium

$$P_2(x_2) = \int dk \int_0^{x_2} dx_1 P_1(x_1) K(k) \delta\left(k - k_f \frac{\ell_f - x_2}{x_2 - x_1}\right) \tag{6}$$

In the above expression we have introduced a delta-function to fix force balance as well as enforcing the inequality: $x_1 < x_2$. Performing the above integral requires further information about the probability distribution of x_1. To do so we note that $P(x_1)$, which represents the displacement modulo ℓ_f of the filamin spring under a constant force, must be independent of the details of the particular sawtooth potential under consideration. It is then reasonable to make the *ansatz* that the distribution of x_1 along the sawtooth is flat:

$$P(x_1) = 1/\ell_f. \tag{7}$$

Using Eq. 7 in Eq. 6 and performing the integral over x_1 we find

$$P(x_2) = \frac{k_f(\ell_f - x_2)}{\ell_f} \int_{k_f \frac{\ell_f - x_2}{x_2}}^{\infty} dk k^{-2} K(k) \tag{8}$$

From this equation for $P_2(x_2)$, it is clear that the exponential nature of the cross-link length distribution is not merely inherent to the sawtooth nature of its force law. The exponential must result from weighted integral over $K(k_{eff})$ and thus depend on the nature of the random network as a whole.

To pursue this point we focus on the high k_{eff} tail of the distribution. One may imagine that the effective spring constant representing the medium can be represented as a small number of chains of springs. Each chain of springs represents one path for force propagation through the random network; it is made up of a large number (N) of springs connected in series. These springs have spring constants of the form: $k^{(\alpha)} \sim \mu / l_\alpha$, where the random variable l_α is the distance between two cross-links measured along the filaments following the path of force propagation in one realization of the network. Because of the random connectivity of the network, we expect these spring constants to be statistically independent and uniformly sample the random distribution of the distances l between cross-links generally found in the network.

In order to find an extremely large value of the effective spring constant k_{eff} we require that at least one of these parallel paths have a large effective spring constant k_j, since $k_{eff} = \sum_j k_j$ where the sum over j runs over the number of parallel paths of force propagation. For some k_j to be large, it must be that the sum of the reciprocals of the spring constants $k_j^{(\alpha)}$ associated with that particular path be small. This requires that for one of the paths j, *all of the constituent spring constants are large* since the compliance of the springs in series will be dominated by any single soft spring. We expect that probability of

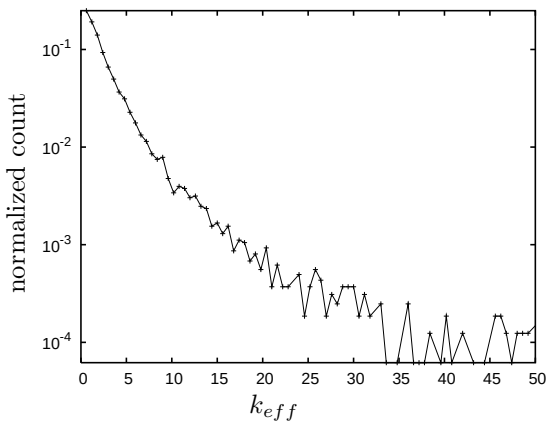

FIG. 5: Distribution of local effective spring constants, sampled on small sets of highly stretched filamin cross-linkers for $k_f = 600$.

such a rare event to be Poisson distributed $K(k) \sim k^N$ so that, in the high-k tail, the distribution $K(k)$ takes the form

$$K(k) \sim H(k)e^{-k/\bar{k}} \tag{9}$$

where H is some regular function characterizing the small-k behavior of the distribution ($H(x) \longrightarrow$ const as $x \longrightarrow \infty$) and the constant $\bar{k}$ is undetermined. Combining Eqs. 9 and 5 we indeed find that the probability distribution of x_2 takes the form

$$P_2(x_2) \simeq Ce^{\frac{k_f(x_2-\ell_f)}{\bar{k}x_2}} - \frac{k_f(\ell_f - x_2)}{\bar{k}\ell_f}\Gamma\left(0, \frac{k_f(\ell_f - x_2)}{\bar{k}x_2}\right) \tag{10}$$

as long as $k_f\frac{\ell_f - x_2}{x_2}$ is large enough that $K(k)$ within the integral in Eq. 8 can be replaced by its high-k asymptotic form. Examining the first term of the above result, we see that we do find the expected exponential peak in the probability distribution at x_2 near the sawtooth length, ℓ_f. The second term, which is proportional to the incomplete gamma function is a subdominant correction to the distribution near the exponential peak at $x_2 \mathrm{mod} \ell_f \rightarrow \ell_f$.

We can turn to the numerical simulations to independently verify some of the underlying assumptions in the above analysis. By numerically sampling the local mechanical response of the many realizations of the network, we find that we can indeed independently verify the principal physical insight in the above discussion: the distribution of effective spring constants appears to have an exponential tail in the stiff spring limit. This data is presented in Figure 5. Moreover, on an ordered triangular lattice of springs where we would not expect to find such a high k exponential tail, one does not find the exponential enhancement of the critical subpopulation[31]. This suggests that details of the random connectivity of our networks play a vital role in producing this phenomenon.

We can also use Figure 5 to estimate the value of $\bar{k}$. Taking into account the highest k_{eff} data for which we were able to sample the mechanical response distribution in a statistically significant manner, we find $\bar{k}$ to be ~ 20. This puts the ratio $k_f/\bar{k} \sim 30$. Using Eq. 10 we may also determine this ratio using the slope of the numerically measured distribution of x_2 shown in Figure 4(b). From fitting this data we find that $k_f/\bar{k} \sim 15$. These values are of the same order of magnitude and the factor of two discrepancy between them may be due in part to the insufficient sampling of the k_{eff} distribution in the rare, high-k_{eff} limit as well as to the effect of the unknown behavior of $H(k)$ (see Eq. 9) at intermediate values of its argument.

IV. DISCUSSION

In this work we have studied a composite network composed of linear elastic elements having randomly distributed spring constants cross-linked by filamin-type linkers that have the ubiquitous sawtooth force-extension relation common to proteins with repeated unfolding domains. While this system is clearly a vast oversimplification of both the chemical complexity and semiflexible character of the cytoskeleton, these networks retain one important micro-architectural feature of the F-actin, filamin networks that are typically found in eukaryotic cells in that forces must propagate from filament to filament through a linking molecule exhibiting a highly nonlinear (sawtooth) force response to strain. We suspect that our model system can thus inform the understanding of the mechanical properties of physiological cytoskeletal networks, which are the subject of recent theoretical work and are being probed experimentally with increasing quantitative accuracy[21, 32].

The most striking result of this investigation is the observation of the development of a highly fragile mechanical state in the highly-strained network such that a nontrivial number of cross-linking molecules reach a critical state where they are poised to unfold another domain. The presence of fluctuating internal stresses in the cytoskeleton produced by molecular motor activity and/or equilibrium fluctuations can act on this highly fragile state to produce large strain fluctuations due to the correlated failure of numerous critical cross-linkers. Thus, the observation of the formation of this critical state under applied stress may explain a particular feature of the observed low-frequency strain fluctuations as observed by intracellular microrheology.

We believe that this work suggests the appropriate theoretical framework for understanding the underlying mechanism by which the system reaches this highly fragile state. We note, however, that much remains to be done in order to develop this understanding into a theory that makes quantitatively accurate predictions. In addition it is clear that more precise numerical explorations of the network are required in order to better characterize both the local elastic constant distribution in the network as well as the filamin length distribution.

It is still an open question as to whether the effective medium spring constant distribution has quantitatively correct exponential tail for creation of the observed critical linker subpopulation. Nevertheless, it appears that the creation of this fragile state is a robust phenomenon. Moreover, the simple theory presented herein is in reasonable agreement with the numerical data; it should serve as starting point for more refined models.

There are a number of extensions of this work that remain to be considered. Foremost among these is the exploration of the effect of filamin-type cross-linkers in semiflexible gels where the filaments each have a finite bending modulus. In addition, the development of a complete model that includes the effect of internally generated random stresses due to the action of molecular motors will be an important step towards the direct calculation of the low-frequency dynamics of this biopolymer gel of fundamental biological importance.

Acknowledgements

BD and AJL thank J.C. Crocker for providing unpublished data and for enjoyable discussions. BD also thanks David Morse for enlightening discussions. AJL was supported in part by nsf-dmr0354113. BD acknowledges the hospitality of the UCLA department of Chemistry and the California Nanoscience Institute where part of this work was done. BD also acknowledges partial support from nsf-dmr0354113 and the Institute for Mathematics and its Applications with funds provided by the National Science Foundation.

[1] B. Alberts, D. Bray, J. Lewis, M. Raff, K. Roberts, and J.D. Watson, *Molecular Biology of the Cell, 3rd edition* (Garland, New York, 1994); P.A. Janmey Curr. Opin. Cell Biol. **3**, 4 (1991).
[2] T.D. Pollard and J.A. Cooper, Ann. Rev. Biochem. **55** 987 (1986).
[3] E.L. Elson Annu. Rev. Biophys. Biochem. **17**, 397 (1988).
[4] M. Rubenstein and R.H. Colby, *Polymer Physics* (Oxford University Press, London, 2003).
[5] P.A. Janmey, S. Hvidt, J. Lamb, T.P. Stossel Nature **345**, 89 (1990).
[6] K. Kroy and E. Frey, Phys. Rev. Lett. **77**, 306 (1996).
[7] R. Satcher and C. Dewey, Biophys. J. **71** 109 (1996).
[8] F.C. MacKintosh, J. Käs and P.A. Janmey, Phys. Rev. Lett. **75**, 4425 (1995).
[9] D.A. Head, A.J. Levine and F.C. MacKintosh, Phys. Rev. Lett **91**, 108102 (2003).
[10] J. Wilhelm and E. Frey, Phys. Rev. Lett. **91**, 108103 (2003).
[11] D.A. Head, F.C. MacKintosh and A.J. Levine, Phys. Rev. E **68**, 025101(R) (2003).
[12] D.A. Head, F.C. MacKintosh and A.J. Levine, Phys. Rev. E **68**, 061907 (2003).
[13] Alex J. Levine, D.A. Head, and F.C. MacKintosh J. Phys.: Condens. Mat. **16**, S2079 (2004).
[14] B.A. DiDonna and T.C. Lubensky Phys. Rev. E *Accepted for publication* (2006).
[15] D.A. Head, A.J. Levine, and F.C. MacKintosh Phys. Rev. E *Accepted for publication* (2005).
[16] M.L. Gardel, J.H. Shin, F.C. MacKintosh, L. Mahadevan, P. Matsudaira, D.A. Weitz Scince **304**, 1301 (2004).
[17] S. Labeit and B. Kolmerer Science **270**, 236 (1995).
[18] M. Rief, M. Gautel, F. Oesterhelt, J.M. Fernandez, H.E. Gaub Science **276**, 1109 (1997).
[19] I. Schwaiger, A. Kardinal, M. Schleicher, A.A. Noegel, and M. Reif Nature Struct. Mol. Biol. **11**, 81 (2004).
[20] D.J. Brockwell, G.S. Beddard, E. Paci, D.K. West, P.D. Olmsted D.A. Smith, and S.E. Radford Biophys. J. —bf 89, 506 (2005).
[21] B.D. Hoffman, G. Massiera, and J.C. Crocker cond-mat/0504051 (2005).
[22] P.R. Onck, T. Koeman, T. van Dillen, and E. van der Giessen cond-mat/0502397 (2005).
[23] J.F. Marko and E. Siggia Macromol. **28**, 8759 (1995).
[24] E. Evans and K. Ritchie Biophys. J. **72**, 1541 (1997).
[25] E. Frey, K. Kroy and J. Wilhelm, in Dynamical Networks in Physics and Biology,ed. D. Beysens and G. Forgacs (EDP Sciences ? Springer, Berlin, 1998).
[26] T. P. Stossel et al., Nature Reviews Molecular Cell Biology **2**, 138 (2001).
[27] Furuike, S., T. Ito, and M. Yamazaki, Febs Letters **498**, 72 (2001).
[28] M. Kellomäki, J. Åström, and J. Timonen Phys. Rev. Lett. **77**, 2730 (1996).
[29] L.D. Landau and E.M. Lifshitz *Theory of Elasticity* 3$^{\rm rd}$ *Ed.* Pergamon Press, Oxford (1986).
[30] B.A. Didonna and A.J. Levine in progress (2006).
[31] J.C. Crocker Private communication (2005).
[32] A.W.C. Lau, B.D. Hoffman, A. Davies, J.C. Crocker, and T.C. Lubensky Phys. Rev. Lett. **91**, 198101 (2003).
[33] The onset of non-linear effects could also occur at smaller strains or even zero strain if the system has high internal stresses, which many physiological systems display in equilibrium. The effects of internal stresses will be explored in future work [30].